

The Relief Canyon Gold Deposit, Nevada: A Mineralized Solution Breccia

ALAN R. WALLACE

U. S. Geological Survey, Mail Stop 905, Box 25046, Denver Federal Center, Denver, Colorado 80225

Abstract

The Relief Canyon gold deposit in the Humboldt Range of western Nevada is a low-grade, high-tonnage orebody of Tertiary or younger age. The host rocks include limestones of the Triassic Cane Spring Formation, which are overlain by shales of the Triassic Grass Valley Formation. The rocks were folded and metamorphosed to greenschist grade during Jurassic and Cretaceous regional tectonic activity. Mesozoic thrusting may have occurred along the shale-limestone contact, but evidence has been obscured by later hydrothermal activity. The sedimentary rocks were nominally offset along several Late Tertiary normal faults related to uplift of the range.

The upper part of the Cane Spring Formation is composed of a poorly sorted breccia composed of limestone clasts with a clay matrix. Irregular pockets within this zone are filled with clay- to pebble-sized fragments derived from the Grass Valley shale. The enclosing limestone beds were tilted moderately to the southwest during Mesozoic deformation, whereas bedding within these pockets is generally horizontal, indicating post-tilting deposition of the sediments. The sediments show graded bedding and other sedimentary features that indicate deposition from flowing water. Thermally mature carbon derived from the limestone is also concentrated in small pockets in the matrix. The breccia unit is likely the product of low-temperature solution brecciation. Ground water dissolved much of the limestone directly beneath the shales, progressively creating irregular cavities and the breccia. Sediments derived from the overlying Grass Valley shale were fluviially deposited as a matrix to the developing solution breccia.

Episodic pulses of hydrothermal fluids were introduced along faults and possibly mixed with the ground water in the breccia zone. Initially, jasperoids formed along the faults, but later hydrothermal pulses introduced gold, silica, and fluorine into both the early jasperoids and the unconsolidated cave-fill sediments to form the orebody. Continued solution-related brecciation chaotically disrupted the gold deposit.

Gold, fluorite, pyrite, silver, calcite, and fine-grained silica are the principal hydrothermal minerals in the deposit. Gold was deposited as micron-sized flakes of native gold and rarely as electrum during a relatively late stage of silicification of the jasperoids, the carbon-rich zones, and the clay-rich matrix of the breccia. Fluorite was deposited with and later than the gold in the jasperoids, and it in part replaced the clay-rich breccia matrix. Antimony, arsenic, mercury, and thallium are directly associated with gold in the orebody.

The deposit formed at a relatively shallow depth. On the basis of fluid inclusion data, late-stage hydrothermal fluids related to gold and fluorite deposition were extremely dilute and had temperatures near 200°C. The fluid inclusions in fluorite show no evidence for boiling, but porous crackle breccias in the jasperoids suggest that hydrobrecciation took place.

Introduction

THE Relief Canyon gold deposit, at the south end of the Humboldt Range and 25 km east of Lovelock, Nevada (Fig. 1), is a variant on the theme of "sedimentary rock-hosted" ore deposits. The deposit is relatively small (8-10 million tons) and has a very low grade (average of 0.03 oz Au/ton), but the occurrence of ore in sediment-filled solution breccias in limestone, as well as in jasperoids, is in part similar to the occurrence of ore in some Mississippi Valley-type base metal deposits.

The site was initially known as the Bohannon fluor-spar prospect, where irregular pods and veins of fluor-spar were mined in the 1940s (Papke, 1979). In 1978, the property was staked for high-purity limestone and one diamond core was drilled to evaluate

the extent of the limestone. An exploration program by Duval Corporation in 1979 detected gold in stream sediments from the site and assays of the core showed the presence of gold (Fiannaca and Eason, 1984). Subsequent surface sampling and drilling delineated the gold deposit that is now being mined. Lacana Mining, Inc., purchased the property in 1982 and began open-pit mining in 1984; Pegasus Gold Company purchased the property in 1986. The western 10 percent of the deposit, which is not currently (1988) being developed, is owned by Southern Pacific Railroad Company. The ore is exploited in an open-pit mine and the gold released by cyanide heap leaching after agglomeration.

Based on detailed bench mapping in the mine and reconnaissance mapping near the deposit, along with

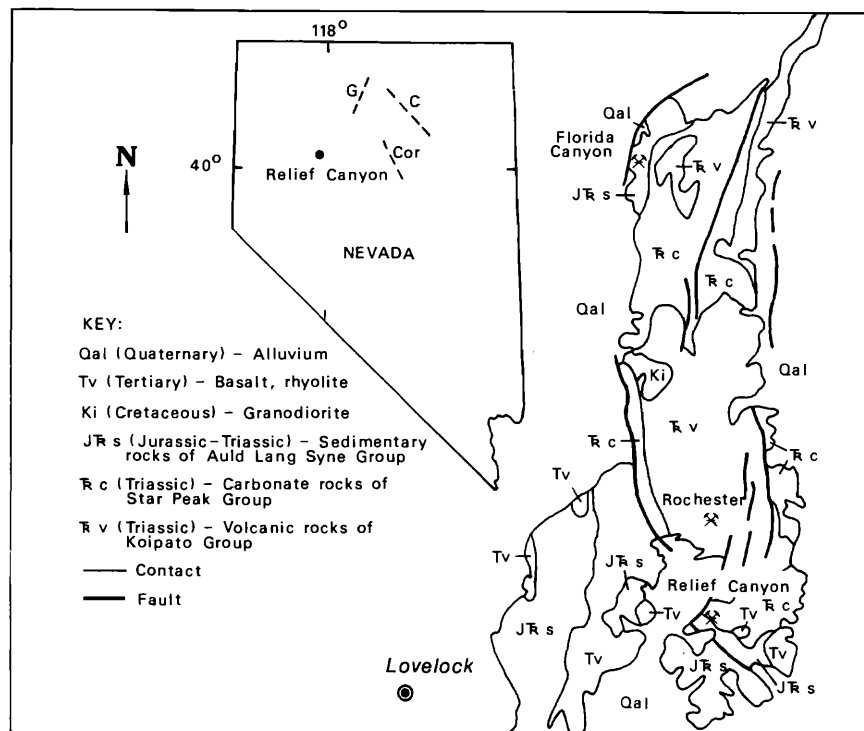


FIG. 1. Location of the Relief Canyon gold deposit in relation to other gold deposits in northern Nevada (inset map) and in relation to the geology of the Humboldt Range. The inset map of Nevada shows major gold trends and deposits: C = Carlin trend, Cor = Cortez trend, G = Getchell trend. On the geologic map of the Humboldt Range, deposits include, from north to south, Florida Canyon, Rochester, and Relief Canyon. Geology simplified from Stewart and Carlson (1978).

the results of initial fluid inclusion and trace element studies, this paper summarizes the geologic relations as exposed in the open-pit mine by June 1987. Study of the deposit will continue as it is exposed. Previous work on the area included regional mapping by Wallace et al. (1969a) and detailed surface mapping and drilling by Lacana and Southern Pacific during initial property evaluation and development (Fiannaca and Easdon, 1984; Wittkopp et al., 1984).

Regional Geologic Setting

The Humboldt Range is a north-trending structural horst that formed during late Cenozoic normal faulting. Thick alluvial fan deposits fill the adjacent grabens. The oldest rocks exposed in the range include mafic to largely silicic volcanic rocks of the arc-related Lower Triassic Koipato Group (Silberling and Wallace, 1967; Wallace et al., 1969a and b; Fig. 1). A carbonate platform (Star Peak Group) developed over the volcanic rocks during Middle Triassic time, and it was succeeded in Late Triassic and Early Jurassic time by a fluvial-deltaic system which deposited sediments of the Auld Lang Syne Group (Silberling and Wallace, 1969; Elison and Speed, 1988). Between Middle Jurassic and Middle Cretaceous time, coeval

basinal sedimentary rocks were thrust southeasterly over the platform and deltaic rocks (Oldow, 1984); all the units were deformed and metamorphosed to at least greenschist grade. Late Cretaceous granitic plutons were emplaced into the Mesozoic sedimentary and volcanic rocks after the Middle Jurassic to Middle Cretaceous deformation. Cenozoic volcanic rocks were erupted over much of the region but were largely eroded during Miocene and younger uplift of the ranges. Isolated remnants of Miocene basaltic and rhyolitic volcanic rocks are exposed in the southern part of the Humboldt Range and in neighboring ranges (Wallace et al., 1969a; Fig. 1).

Geology

The Relief Canyon gold deposit formed in a limestone solution breccia unit which developed at the contact between the Upper Triassic (Karnian) Cane Spring Formation of the platform assemblage and the overlying Upper Triassic (Norian) Grass Valley Formation of the fluvial-deltaic assemblage (Figs. 1 and 2). The sedimentary rocks dip moderately to the southwest. Prior to mining, the breccia unit was exposed between the massive limestone outcrops and the less distinct Grass Valley exposures, as well as in

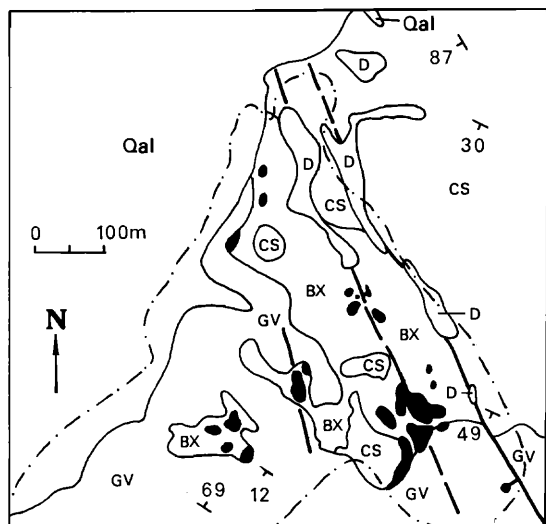


FIG. 2. Surface geology of the Relief Canyon gold deposit prior to mining. Modified from Fiannaca and Easdon (1984) and unpublished Lacana Mining, Inc., mapping. Approximate outline of open-pit mine is delineated by dot-dash. Other units: black areas = jasperoid, BX = breccia unit, CS = Triassic Cane Spring Formation, D = Mesozoic (?) diabase, GV = Triassic Grass Valley Formation, Qal = Quaternary alluvium.

small windows in the overlying Grass Valley (Fig. 2). Diabase dikes of probable post-Late Cretaceous age fill northwest-trending faults on the eastern margin of the deposit. High-angle northwest-trending faults also cut the sedimentary rocks.

Host rocks

Cane Spring Formation: The Cane Spring Formation is characterized by a very thickly bedded limestone sequence that forms the upper part of the Triassic Star Peak Group (Nichols and Silberling, 1977). At and adjacent to the mine, beds of the Cane Spring are light gray to bluish black, locally pyritic limestone as much as 4 m thick. Bedding-parallel stylonitic layers contain sooty black carbonaceous material and residual quartz grains. The limestone is predominantly micrite and fossiliferous micrite with interbedded silty micrite and biosparite. Local dolomitization produced patches of coarse-grained dolomite (Fig. 3A). Due to the extensive development of the solution breccia, the limestone exposed at the mine is limited to small islands of coherent rock. The lower part of the formation, exposed north of the mine, is thinner bedded (less than a meter thick) and contains conglomerate and quartzofeldspathic interbeds.

Grass Valley Formation: The Grass Valley Formation, the lowest part of the Auld Lang Syne Group, consists of olive-gray argillite, siltstone, and tan sandstone and it depositionally overlies the Cane Spring Formation. The blue-gray argillites and siltstones

contain subangular to subrounded quartz grains with interstitial potassium micas and chlorite (Fig. 3B). The sandstones are composed of quartz, micas, and iron oxides and a quartz-overgrowth cement.

The contact between the Grass Valley and the Cane Spring is poorly exposed in outcrop. As exposed in the mine, the contact has been modified by solution-related brecciation. The unmodified contact, where exposed in the mine and outside the deposit, appears to be conformable.

Dikes: Pervasively altered diabase dikes fill vertical, north-northwest-trending fault zones along the northeast side of the deposit; exposures extend for more than 1,200 m. The dikes are composed of phenocrysts of plagioclase and pyroxene, which have been altered to sericite, chlorite, carbonates, and iron oxides, in a very fine grained altered groundmass; as a result of alteration and oxidation, the dikes are a bright orange color at the mine. Similar dikes are widely distributed throughout the Humboldt Range, and they cut rocks as young as Late Cretaceous in age (Wallace et al., 1969b); however, the absolute age of the dikes is unknown.

Altered, fine-grained monzogranite dikes were encountered in rotary drill holes (Wittkopp et al., 1984), but none had been exposed during mining by early 1988.

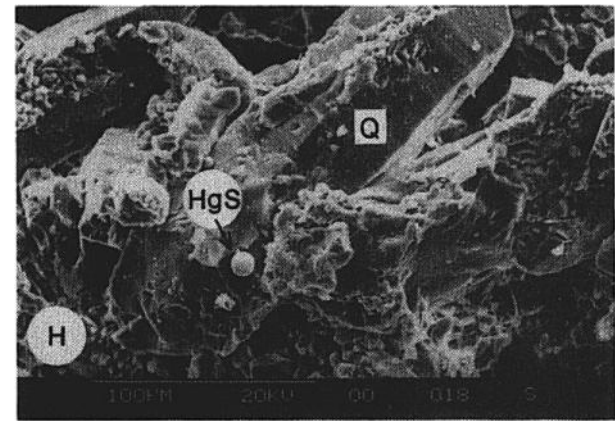
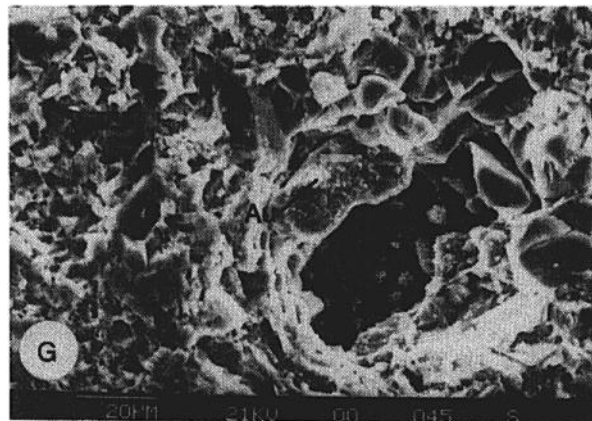
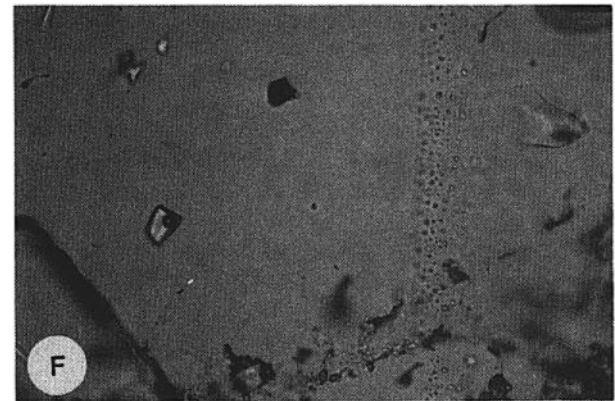
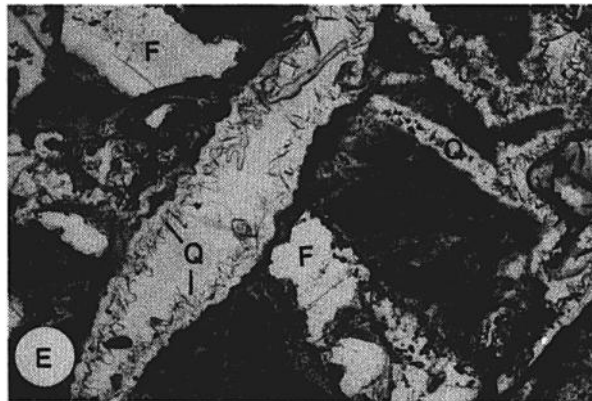
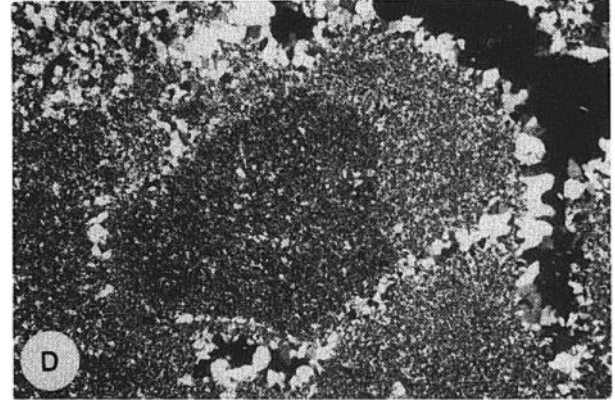
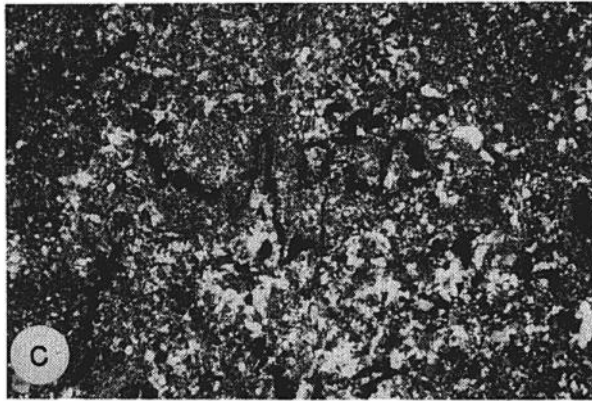
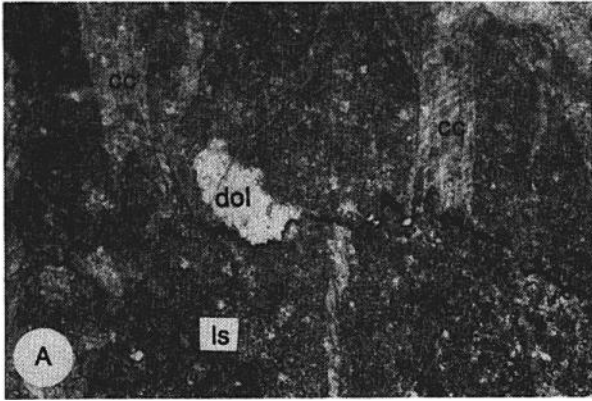
Structure and metamorphism

Mesozoic deformation: The sedimentary rocks were metamorphosed to lower greenschist facies during regional Jurassic and Cretaceous deformation (Oldow, 1984). Mesoscopic to map-scale northwest- and northeast-trending isoclinal folds are common in the Cane Spring Formation less than a kilometer to the northeast of the mine, whereas the limestone beds at the mine dip relatively uniformly to the south-southwest. The Grass Valley Formation is complexly folded and faulted both at the mine and in surface exposures to the south.

Penetrative slaty cleavage in both the Grass Valley and Cane Spring Formations imparts a distinct platy texture that is oblique to bedding. Slaty cleavage is particularly well defined in the Grass Valley, where it generally obscures the bedding. Cleavage is poorly developed in the massive Cane Spring limestones, although it is well defined in shaly interbeds.

Postcleavage stylonites are common at all scales in the Cane Spring limestones and at a microscopic scale in the Grass Valley shales. The stylonites sever veins of calcite and quartz in the limestones and shales, respectively, suggesting some pre- or syndeformation vein development. The stylonites also truncate patches of coarse-grained dolomite (Fig. 3A).

Cenozoic structures: Several north-northwest-trending high-angle fault and fracture zones traverse the deposit. At least one fault zone is occupied by an



altered diabase dike; silicification along several of the others produced tabular jasperoid bodies (Fig. 2). The faults are, by themselves, indistinct; where they cut the Grass Valley in the mine, the rocks are broken into angular, centimeter-size fragments. Rotary drilling records show several discontinuous, northwest-trending zones across which the base of the Grass Valley Formation has been downdropped a total of 10 to 20 m to the northeast. Linear jasperoid bodies conform to some of these small faults. The diabase dike is weakly sheared along its margins, indicating some late movement along the host fault, but the dike appears to have been emplaced largely after the fault formed. Outcrop patterns indicate that the western side of that fault was downdropped (Fig. 2).

The range front north of the mine slopes precipitously to the west and is cut at its base by a high-angle, north-northeast-trending normal fault, which has hundreds of meters of apparent vertical offset related to Tertiary and younger uplift of the range (Fig. 1). In contrast, the range front south of the mine is subdued and the frontal zone is much less pronounced. This in large part may be due to a southward change from resistant limestones to more readily eroded shales. However, on the basis of rotary drilling data, a structure contour map of the base of the Grass Valley shows that the contact dips moderately to the west with no pronounced offset across the southwest projection of the range-front fault (Lacana Mining Co., unpub. data). As the topographic change in the range front occurs approximately where the north-northwest-trending faults exposed in the mine intersect the northeast-trending range front, uplift of this part of the range may have been facilitated by movement along one or more of those faults. If so, this suggests that these faults, which are genetically related to mineralization, are of mid-Tertiary age or younger.

Joints in the Cane Spring limestone are predominantly west-northwesterly and have steep dips to the southwest and northeast. Limestone dissolution along these surfaces is visible throughout the deposit and likely facilitated the formation of the breccia.

Breccia unit

At the Relief Canyon gold deposit, limestones of the Cane Spring Formation immediately beneath the Grass Valley Formation were partially reduced to an unconsolidated, poorly sorted rubble of subrounded limestone fragments in a matrix of silt and clay (Fig. 4). In places, the Grass Valley beds have collapsed as much as 40 m into large, pipelike cavities, forming a chaotic jumble of small fragments. On the basis of drilling data, the breccia zone is generally 30 to 70 m thick, but it ranges from less than 10 m to more than 100 m thick. Most of the limestone fragments vary from a centimeter to more than a meter in diameter. Coherent limestone blocks tens of meters or more in dimension are exposed in the mine directly beneath the Grass Valley Formation or as islands in the breccia. On the basis of rough visual estimates in the mine, at least a third of the original limestone in the breccia zone was dissolved.

The matrix of the breccia is composed of clay- to pebble-sized fragments of the Grass Valley Formation. Larger fragments of the shale are locally abundant near the Grass Valley-Cane Spring contact. Both compaction and drape textures are evident in the interstitial clays, suggesting that the clays were in part deposited during formation of the collapse zones. Most of the breccia fragments are clast supported, but pockets of clay several meters across are not uncommon.

Irregular solution cavities permeate the unbrecciated limestone. The cavities are along joints or less commonly along bedding planes in the limestone, and

FIG. 3. Photomicrographs of host rocks and ores. A. Cane Spring Formation limestone (ls), with diagenetic patchy dolomite (dol) and calcite veinlets (cc); veinlets cut dolomite elsewhere in the sample. Calcite and dolomite are truncated by stylonite, along which carbonaceous material was concentrated. Width of field of view equals 1.16 mm. B. Foliated Grass Valley Formation shale, with folded calcite veinlet (cc; outlined). Short inked lines parallel foliation direction. Width of field of view equals 2.45 mm. C. Relict stylonite in replacement jasperoid body in limestone. Width of field of view equals 2.45 mm. D. Three generations of jasperoid, including darker, finer grained early jasperoid in center, medium gray and medium-grained intermediate-stage jasperoid, and late vug-filling, coarser jasperoid; black area on upper right is a vug. Gold is usually associated with the later and, in places, the intermediate, stages of jasperoid. From tabular jasperoid body along fault zone. Width of field of view equals 2.45 mm. E. Early jasperoid (dark), cut by quartz (Q) and fluorite (F) veinlets, with late vuggy quartz veinlets. Elsewhere in sample, fluorite and the first generation of quartz veinlets are mutually crosscutting, and gold is associated with the quartz veinlets. Width of field equals 2.45 mm. F. Large liquid-vapor primary fluid inclusion (left) and two-phase secondary inclusions along a fracture (right). Width of field of view equals 0.58 mm. G. Scanning electron microscope view of 4- μ m flake of gold (Au) resting on an incompletely filled vug in porous jasperoid. All other material in photograph is fine-grained quartz. Scale shown at bottom of photograph. H. Scanning electron microscope view of mercury sulfide (HgS; cinnabar?) on euhedral, late-stage quartz (Q) in silicified cave-fill sediments. Submicron-size gold is associated with this stage of mineralization in this sample. Scale shown at bottom of photograph.

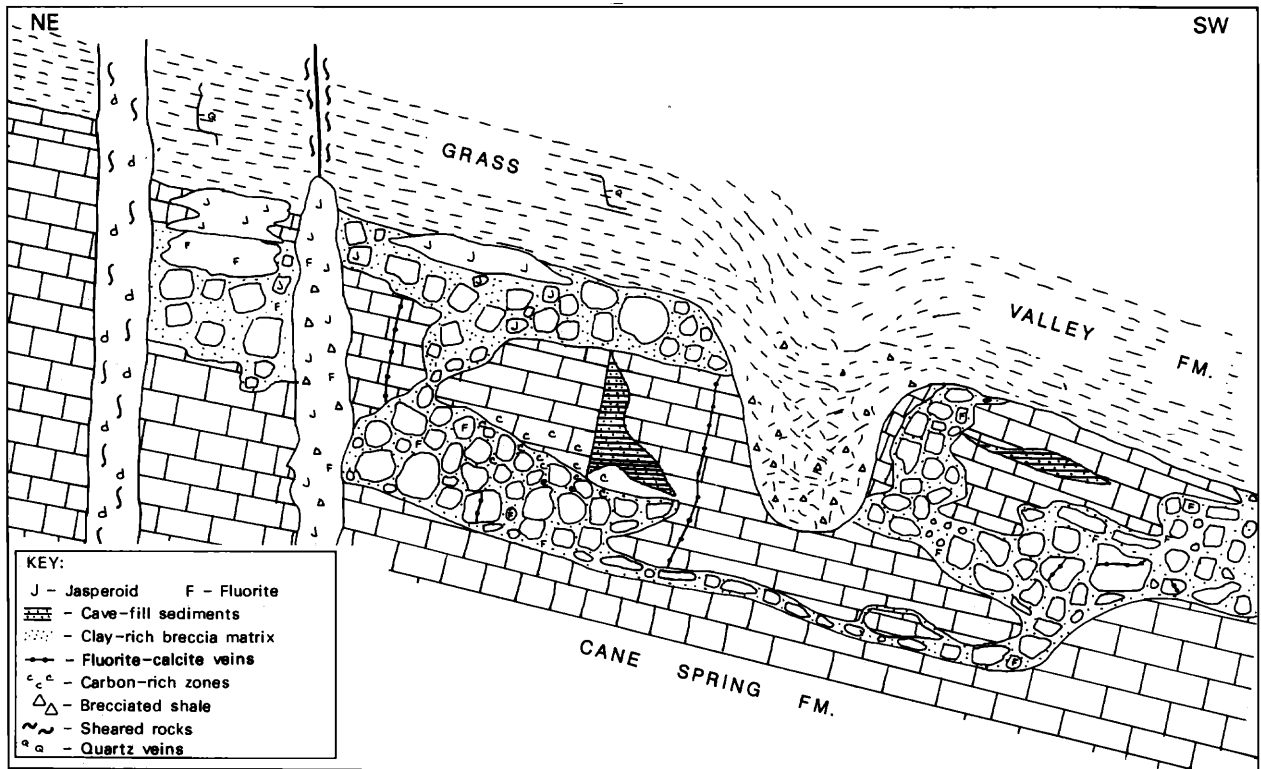


FIG. 4. Schematic cross section looking southwest through breccia zone in Cane Spring Formation. Section drawn to show general relations between host rocks, breccia, collapse structures, and veins. The breccia matrix, cave-fill sediments, jasperoids, and some of the collapsed Grass Valley shale are mineralized and contain gold. All unlabeled breccia fragments are composed of limestone. Fluorite (F), where not in breccia fragment, replaces breccia matrix or jasperoid; d = diabase dike. Section not drawn to scale.

they are filled with clastic sediments. Most of the sediments are clay to silt sized, but some include fine, subrounded pebbles of Grass Valley siltstone and shale. The sediments show graded bedding and other fluvial-related depositional textures. Bedding is roughly horizontal, in contrast to the southerly dip of the surrounding limestone, indicating that deposition of the sediments occurred after tilting of the host rocks.

Limestone beds and limestone breccias both abut the large diabase dike. When its well-defined, tabular form is considered, the dike was probably emplaced prior to solution brecciation and it follows that the original fault in which it occurs is also older than the breccia. Similarly, linear jasperoid bodies fill fault zones that pass through the incoherent breccia, suggesting that the faults and at least the early jasperoids formed prior to brecciation. Indeed, jasperoid fragments are present in some breccia zones and less commonly in the bedded cavity-filling silts.

The breccia unit had been described previously as a subaqueous debris flow ("fluxoturbidite"; Fiannaca and Eason, 1984) that formed during Triassic shelf-slope sedimentation and as a thrust-related breccia

(Wittkop et al., 1984). However, metamorphic fabrics in the clasts indicate a postmetamorphic (post-Jurassic-Cretaceous) age for brecciation. Although earlier thrusting may have occurred along the contact, textures in the breccia indicate contemporaneous formation of the breccia and fluvial deposition of sediments.

Carbon-rich zones

Locally large areas within the breccia zone have a sooty black to gray carbon-rich matrix which resembles and was probably derived from material in the carbonaceous stylonite zones in unbrecciated limestone. In addition, small solution cavities in carbonaceous limestones contain stratified and graded sediments with abundant silt-sized grains of carbon, shale, and limestone.

The Ore Deposit

The major events in the formation of the gold deposit are, in general paragenetic order, faulting, formation of massive jasperoids, solution brecciation of the limestone and fluvial deposition of clays and silts, continued silicification of jasperoids and the clay-silt

breccia matrix, clay-fluorite veining and alteration, and oxidation. Gold was deposited in jasperoids and in the interstitial clays and silts during the later stages of silicification. Mineralogically, the deposit is very simple and is dominated by fine-grained silica, calcite, fluorite, and clay minerals. Pyrite and gold, although important, are extremely rare.

Preore mineralization

Several generations of calcite veins formed in the limestone prior to and possibly during solution brecciation. Irregular zones of coarse white to pink calcite truncate calcite veinlets related to Mesozoic deformation. Closely spaced veinlets (<1 mm) of clear calcite cut the limestone breccia fragments and domains between the veinlets are bleached and partially dolomitic. Vuggy veins of coarse calcite cut both fresh and altered limestone. Limited surface exposures show jasperoid veinlets cutting early calcite veinlets, and a few calcite veinlets of unknown paragenetic position cut the jasperoid.

Jasperoids

Gold-bearing jasperoids form tabular bodies along high-angle faults and irregular pods near the shale-limestone contact. The fault-controlled jasperoids are massive to porous and they show evidence of episodic brecciation and resiliification. The contact-related jasperoids are generally less massive and more porous and they form blankets in the limestone beneath the impermeable shale.

Silicification replaced the host rocks (Fig. 3C) and filled close-packed fault breccias with fine-grained silica. The earlier stages of silicification produced very dark, massive jasperoids which contain finely disseminated 1- to 10- μm grains of pyrite, as measured with a scanning electron microscope. Subsequent silicification accompanied repeated brecciation and generated progressively lighter gray, coarser grained, and more porous jasperoids (Fig. 3D). As described below, gold was deposited during one of the later stages of silicification. Late brecciation, perhaps related to hydrofracturing, formed irregular pods and vertical pipes of shattered jasperoid in both fault- and contact-related jasperoids. These breccias are heavily iron stained and incompletely cemented by light-gray silica.

Silicification both preceded and followed the formation of the solution breccia. The dark, massive, fine-grained jasperoids largely formed before solution brecciation. The solution breccias contain scattered fragments of dark jasperoid and collapse of contact-related jasperoid into breccia zones is locally evident. However, later silicification of the clay matrix may have been related to one or more of the later stages of silicification visible in the jasperoids.

Fluorite mineralization

Purple to green fluorite was deposited in jasperoids (Fig. 3E), in vugs and veins in the limestone, and in the clay-rich breccia matrix. Some fluorite formed during relatively early silicification and was replaced or cut by later stages of jasperoid. However, fluorite deposition generally followed most or all major stages of silicification. Irregular pods and discontinuous veinlets cut the massive jasperoids and euhedral fluorite crystals partially fill voids in the porous jasperoids. Fluorite locally occurs in jasperoid veinlets that contain gold, but fluorite also formed in the succeeding stage of mineralization. Granular to massive fluorite-calcite pods are irregularly distributed beneath and replace the contact-related jasperoids and adjacent breccia matrix. Fractures, joints, and vugs lined with coarse, euhedral fluorite and calcite cut fresh limestone.

Fluorite commonly forms small euhedral grains to 5-cm nodules with calcite in the breccia matrix. Concentric color zoning in the nodules and most grains suggests growth in place. In contrast, fragment borders of some smaller grains cut color zoning, suggesting postdeposition brecciation and incorporation into the matrix. The solution breccia also contains fragments of fluorite-bearing limestone and jasperoid, indicating at least some postfluorite solution brecciation.

Postbreccia mineralization

Silica and calcite both replace and cement the matrix of the breccia. Calcite veinlets also cut the silicified matrix. Scanning electron microscope studies show that the quartz forms 1- to 5- μm platelets in the matrix and 10- to 40- μm euhedral crystals that project into small voids and pore spaces, a texture similar to that found in the jasperoids. As described below, gold and sulfides locally form micron-sized flakes on the surfaces of these crystals.

The breccia matrix is composed largely of clay-sized particles of both detrital and authigenic origin. White to yellowish 2M₁ hydrothermal clays visibly replace the breccia matrix, jasperoids, and the Grass Valley shales. However, on the basis of X-ray diffraction studies of various clay size fractions, no mineralogic distinction could be made between detrital and hydrothermal clays in the matrix.

Postmineralization dissolution of the limestone generated irregular caves as much as several meters in maximum dimension that cut calcite-fluorite veins. The cavities do not contain cave-fill sediments and are lined with a thin layer of white, botryoidal calcite.

Oxidation

The breccia matrix and some of the jasperoids and host rocks have been partially to completely oxidized. Yellowish-orange oxidation rinds around weathered

fragments of shale in late collapse zones indicate at least some supergene oxidation, but hypogene hydrothermal or supergene oxidation generally cannot be differentiated. Virtually all the breccia matrix is oxidized to bright orange to yellow colors, whereas most of the limestone fragments are dark gray. Well-defined oxidation fronts are visible in the Grass Valley shales in which diagenetic pyrite and most of the chlorite were destroyed. Some closely packed, matrix-poor limestone breccias are extremely hematitic and the hematite is oxidized to limonite. Rare, small cubic voids in the strongly oxidized clay matrix may represent casts of pyrite grains and some of the pyrite in jasperoids have partially oxidized rims.

Oxidation of the black carbon-rich matrix of the breccias largely destroyed carbonate fragments and pyrite. The oxidation front between black and yellow clays is locally marked by a thin reddish zone of hematite.

Trace Elements

Trace element data for the deposit are summarized in Table 1. Gold occurs principally in jasperoids and the silicified clay matrix of the solution breccia; the carbon-rich clay matrix also contains economic gold values. The gold is accompanied by arsenic, mercury, antimony, and some silver, a suite typical of many epithermal gold deposits (Silberman and Berger, 1985). Fluorine is anomalously high in all mineralized rocks and lithium is slightly anomalous in the jasperoids and noncarbon clays. Arsenic and gold values correlate in the jasperoids but not in the clays, where arsenic, mercury, and antimony are more closely associated. Similarly, slightly elevated thallium values occur in the clay matrix, especially the carbon-rich zones where higher values parallel increases in arsenic, antimony, and mercury. The concentrations of copper, lead, barium, and zinc in mineralized rocks

are anomalous relative to the limestones but comparable to those in unmineralized Grass Valley shales and siltstones.

Occurrence of Gold and Other Metals

Gold is present in the jasperoids and in the matrix of the solution breccia, including the carbon-rich zones, based upon studies with the scanning electron microscope. In all of the jasperoids, gold occurs as 0.4- to 4.0- μm flakes intergrown with or deposited on fine-grained silica. Gold was not detected in the massive, dark-colored early jasperoids but rather was found in the somewhat coarser grained veinlets and zones that cut the massive jasperoid. Pyrite and galena were deposited in the early jasperoids; gold was not detected in pyrite at the detection limit of the scanning electron microscope. In the later jasperoids, gold occurs in jasperoid veinlets and pods that formed during the later stages, in places the last stage, of silicification (Fig. 3G). Cinnabar, native silver, and arsenic sulfides, as well as rare barium, copper, and tungsten minerals were also detected in the same silica matrix that contains the gold. One grain of silver enveloped a 1- μm flake of a calcium-tungsten mineral, possibly scheelite. Sphalerite and silver sulfides are present in both early and late jasperoids.

Gold in the silicified and oxidized breccia matrix forms 1- μm platelets on quartz and is disseminated through the clay-quartz matrix. Where the matrix is weakly to strongly silicified, gold particles rest on platelets of microcrystalline quartz and on the crystal faces of euhedral 10- μm quartz crystals that project into small voids; mercury sulfides have a similar occurrence (Fig. 3H). The matrix also contains rare grains of barite and various sulfur-free silver and copper minerals.

Gold in the carbon-rich matrix forms 0.5- to 10- μm grains that were deposited on the surface of fine-

TABLE 1. Summary of Trace Element Data (averages) from Ore Zones and Unmineralized Host Rocks, Relief Canyon Gold Deposit, Nevada
All values in parts per million (ppm).

Rock or ore type	No. of samples	F	As	Hg	Sb	Au	Tl	Ag	Ba	Cu	Li	Pb	Zn
Host rocks													
Limestone	9	200	11	0.8	7	<0.1	0.14	<2	15	3	3	<4	23
Shale	4	700	8	0.14	6.7	<0.1	1.1	<2	275	21	41	5	36
Ore zones													
Jasperoid	9	2,700	310	1.3	153	3.2	1.1	11	93	17	115	14	76
Carbon matrix	5	2,200	508	16	174	0.76	13	3	94	20	49	18	95
Clay-silt matrix	10	4,400	561	19	291	1.8	3.8	5	129	21	92	16	79
Fluorite-calcite pod	1	8,900	230	6.6	360	1.7	1.7	3	42	10	130	15	77

Analytical techniques: specific ion electrode (F), hydride generation atomic absorption spectrometry (As, Sb), cold vapor atomic absorption (Hg), bromide digestion atomic absorption (Au), graphite furnace atomic absorption (Tl), induced coupled plasma (Ag, Ba, Cu, Li, Pb, Zn)

grained silica, potassium mica, calcite, and euhedral quartz. Euhedral pyrite cubes, 2 to 4 μm in size, are dispersed through the matrix but are not related to the gold. Trace amounts of galena and one grain of electrum were also detected.

Age of Mineralization

The absolute age of the deposit is unknown, but geologic constraints suggest that mineralization was Tertiary or younger. Pre-Late Cretaceous deformation and metamorphism of the host rocks (Oldow, 1984) preceded the formation of the jasperoids and solution breccia, since foliated and metamorphosed limestone and shale are replaced by jasperoid and are also present as fragments in the breccia. Similarly, the generally horizontal bedding in the mineralized cave-fill sediments implies that sedimentation occurred after major southward tilting of the host rocks. Mid-Tertiary volcanic rocks in adjacent ranges dip moderately to the east (Wallace et al., 1969a; Hudson and Geissman, 1987) and overlying mid-Miocene basalts, including flows on the eastern side of the range, dip to the east, suggesting progressive eastward tilting of the Humboldt and adjacent ranges since mid-Ter-

tiary time. Therefore, the horizontal cave-fill sediments qualitatively suggest a late Tertiary or younger age for the deposit, similar to that of the Florida Canyon deposit along the northwest flank of the Humboldt Range (Vikre, 1984; Vikre and McKee, 1985; Fig. 1).

Many of the ore deposits in the Humboldt Range are concentrically zoned around a 71-m.y. two-mica granodiorite in the west-central part of the range. Vikre and McKee (1985) have argued that mineralization was related to intrusion of this stock. The Relief Canyon deposit, however, is well outside the halo of gold deposits and may not be related to the Cretaceous metallogenic event.

Temperature, Salinity, and Pressure

Fluid inclusion data

Homogenization temperature and freezing-point depression data were obtained from fluid inclusions in metamorphic quartz veins in the Grass Valley Formation and from hydrothermal fluorite and calcite. The data are listed in Table 2. All inclusions are two-phase water inclusions; the vapor phase occupies 10

TABLE 2. Fluid Inclusion Data, Relief Canyon Gold Deposit, Nevada

Sample no.	No. and type of inclusion	Mineral	Salinity (wt %)	T_e ($^{\circ}\text{C}$)	T_h ($^{\circ}\text{C}$)	Comments
5RC100	2, P	Quartz	6.0–6.1	–38	201–208	Metamorphic quartz veinlet in Grass Valley Formation
	1, S	Quartz	6.7	–32	176	
5RC60A	4, P	Calcite	0.1–1.0		151–196	Calcite veinlets in fresh limestone
	1, S	Calcite	0.1		199	
5RC60B	2, P	Calcite	0.17		160–186	Calcite vein in fresh limestone; cuts sample 5RC60A
5RC32B	4, P	Calcite	0.34–0.5	–32 (?)	185–196	Calcite vein in altered limestone fragment
5RC61	5, P	Calcite (inner)	0.17–0.85		168–173	Zoned calcite vein in limestone breccia fragment
	2, P	Calcite (outer)	0.35–1.4		173–181	
5RC57A	5, P	Fluorite	0.1–0.4		192–200	Fluorite in jasperoid
	5, S	Fluorite	0.1–0.4		166–196	
5RC1B	2, P	Fluorite	0.4–0.7		195–201	Fluorite replacing jasperoid
	6, S	Fluorite	0.9–1.0		165–181	
5RC1A	5, P	Fluorite	0.17	–24	225–231	Core of zoned crystal in clay matrix
	2, P	Fluorite	0.17		209–211	
	10, S	Fluorite	0.17	–32	176–218	
5RC14	1, P	Fluorite	0.5	–6.2	202	Fluorite pod replacing clay matrix
	6, S	Fluorite	0.35–0.7		162–184	
5RC20	4, P	Fluorite	0.17–0.35		194–205	Fluorite-calcite pod replacing jasperoid
	4, PS	Fluorite	0.35–0.5		181–187	
	4, S	Fluorite	0.35–0.5		161–173	

Types: P = primary, PS = pseudosecondary, S = secondary

T_e = eutectic temperature (first observed melting), T_h = homogenization temperature, uncorrected for pressure

Note: all inclusions measured contained two-phase water inclusions; vapor bubble occupied 10 to 15 percent of the volume; salinity is listed in equiv wt percent NaCl, based upon freezing point depressions and calculations using Potter et al. (1978)

to 15 percent of the volume. The samples were heated slowly and homogenization temperatures were progressively measured on those inclusions that homogenized first. Freezing point depression measurements were largely made after heating runs; remeasurement of a number of homogenization temperatures after freezing reproduced the initial results, indicating that the inclusions did not stretch. All measurements were made using a Fluid Inc. modified USGS gas-flow stage.

Small, isolated quartz veins which formed during Mesozoic deformation cut the Grass Valley siltstones; samples were collected 1 km south of the mine. Uncorrected homogenization temperatures are 201° to 208°C. The salinity is approximately 6 equiv wt percent NaCl; a depressed eutectic of between -32° and -38°C suggests some divalent cations as well as sodium.

Primary fluid inclusions in fluorite that replaced jasperoids in vugs and veins have homogenization temperatures of 191° to 201°C and salinities between 0.1 and 1.0 equiv wt percent NaCl; secondary inclusions along fractures are somewhat cooler (165°–196°C) but have similar low salinities (Fig. 3F). Primary inclusions in fluorite that replaced the breccia matrix have very low salinities and temperatures of 202° to 231°C; temperatures in one zoned crystal decreased from 231°C in the core to 209°C at the rim. Secondary inclusions homogenized between 162° and 218°C. Vertical or lateral thermal gradients were not apparent from the data.

Rare fluid inclusions were observed in samples of late-stage jasperoid, but they were too small to provide useful temperature data. The inclusions are two-phase, liquid-dominated aqueous inclusions with bubble volumes of approximately 10 to 20 percent. Fluid inclusions were not detected in the earlier jasperoids, largely due to the fine-grained texture.

Several generations of calcite veins cut the limestone breccia fragments. Fluid inclusion homogenization temperatures range from 150° to 200°C in early veins to 160° to 196°C in subsequent veins. Salinities in all inclusions are less than 1.0 equiv wt percent NaCl. Temperatures and salinities in one zoned vein increased slightly from the vein margin (early) toward the center (later), but they fell within the ranges of the other veins.

Pressure and depth estimates

Pressure corrections for metamorphic quartz veins are limited by the vague information on metamorphic conditions and on whether the veins formed under prograde or retrograde conditions. Carbon maturation data described below suggest that the Cane Spring limestones were heated above 300°C during metamorphism and the presence of pyrophyllite in the Grass Valley shales implies that temperatures did not exceed 400°C (Winkler, 1974). The fluid inclusion

homogenization temperatures of 200° to 208°C, therefore, require a pressure-related temperature correction of roughly 100° to 200°C to reach this 300° to 400°C range. With a 6 wt percent salinity, this corresponds to a pressure of approximately 1,200 to 2,000 bars during metamorphism and vein formation (Potter, 1977).

An estimate of the depth of gold mineralization is largely dependent on the age of the deposit, which geologic evidence suggests is late Cenozoic. Mid-Miocene basalts on the east side of the range were erupted onto a paleosurface that now dips 10° to the east. The gross westward projection of this irregular surface over the mine indicates that the site of the gold deposit may have been less than a kilometer below the paleosurface. If the deposit is younger than the basalts, then this provides a maximum depth for mineralization. At the other extreme, the uniform liquid/vapor proportions in fluid inclusions in fluorite argue against boiling, thereby requiring a minimum depth of 100 m (Haas, 1971). However, hydrothermal breccias in the jasperoids suggest that some boiling probably did occur, although the causative mechanisms are unknown. Lacking better information on the age of the deposit and on boiling during gold deposition, these depth estimates indicate minimal (less than 10°C) pressure corrections for inclusions in the hydrothermal calcite and fluorite.

Carbon

Six samples of fresh shale and limestone (including one sample collected 2 km from the mine) and of the black breccia matrix were analyzed for weight percent organic carbon and sulfur. They were then analyzed by Rock-Eval pyrolysis for hydrogen and oxygen indices and for information on thermal maturation (Tissot and Welte, 1984). The results are summarized in Table 3.

The combined Rock-Eval and fluid inclusion data identify a two-stage thermal history for the area of the deposit. The limited Rock-Eval analyses suggest

TABLE 3. Rock-Eval Pyrolysis Results for Host Rocks and Carbon-rich Matrix

Sample no.	Lithology	S (%)	C _{organic} (%)	HI	OI	T°C (max)
5RC10	Limestone	0.02	0.21	28	80	409
5RC28	Shale	0.89	0.14	35	21	496
5RC29	Limestone	0.06	0.09	22	88	528
5RC34	Carbon matrix	1.90	1.00	7	9	431
5RC35	Carbon matrix	2.92	0.62	14	14	528
5RC36	Carbon matrix	3.37	0.41	320	25	498

HI = hydrogen index, OI = oxygen index (Tissot and Welte, 1984)

Analyst: Ted Daws, U.S. Geological Survey

that all of the carbon was heated to temperatures above 300°C (J. Leventhal, oral commun., 1986), presumably during Mesozoic metamorphism. In contrast, fluid inclusion data show that late-stage fluorite mineralization occurred at temperatures near 200°C. Therefore, the carbonaceous material in the breccia matrix was thermally mature when it was mechanically concentrated during solution brecciation of the Cane Spring limestone.

Formation of the Deposit

Geologic evidence cited above has shown that several hydrothermal events have occurred, leading from the early formation of jasperoids through dissolution of the limestone, with attendant cave-fill sedimentation, to silicification and later oxidation. Solution brecciation of the limestone may have been a relatively continuous process which was repeatedly interrupted by pulses of hydrothermal fluids, forming early massive jasperoids and later generating the low-grade gold deposit at a relatively late stage of silicification. As such, the breccia may have been a zone of fluid mixing between cool ground waters and the gold-bearing hydrothermal fluid. However, whether these events represent a continuum or are widely separated in time is unclear, due largely to the chaotic jumble of the mineralized breccia.

The limestone breccia closely resembles those associated with many Mississippi Valley-type deposits (Sass-Gustkiewicz, 1983; Olson, 1984; Rhodes et al., 1984). However, with the exception of the carbon-rich zones, the detrital fraction of the breccia matrix was derived from the Grass Valley Formation and is not a limestone residue. Textures indicate that the detrital Grass Valley fragments were in part deposited from flowing ground water in the developing breccia. The sediments were then weakly silicified, mineralized, and later oxidized.

A few chemical limits can be placed on the mineralizing environment. Temperatures of the dilute fluids that precipitated fluorite and gold were approximately 200°C, dropping slightly to 160°C during the very latest stages of mineralization. Although the potassium concentration is unknown, the preservation of detrital muscovite and the formation of 2M₁ potassium micas qualitatively places the pH in the muscovite-sericite stability field, which at 200°C has a relatively neutral to slightly acidic pH. Partial dissolution of quartz during fluorite precipitation suggests a progressively increasing pH. Early pyrite deposition in the jasperoids and carbon-rich cave-fill sediments occurred in the pyrite stability field, implying a relatively lower oxidation state. The lack of detectable iron in the only identified arsenic mineral indicates a relatively high sulfur fugacity (Rytuba, 1985). Under these general chemical parameters, gold was likely transported as a bisulfide complex (Seward,

1973); fluorine was probably complexed with sodium or calcium (Richardson and Holland, 1979).

The massive, fault-related jasperoids formed early, after which much of the solution brecciation and cave-fill sedimentation may have occurred. Paragenetic relations in the jasperoids and the breccia matrix indicate similar late-stage gold-bearing quartz and associated mercury-arsenic mineralogies, suggesting one late-stage episode of gold deposition. The gold-bearing quartz assemblage in both the jasperoids and the clay matrix was followed or locally accompanied by fluorite deposition. Fluorite-calcite and some calcite veins in the limestone may have formed along joints at the same time. After gold mineralization, continued or renewed brecciation of the limestone, as well as disruption of part of the original breccia matrix, would explain jasperoid and fluorite fragments in the matrix as well as limestone blocks with fluorite-calcite veins.

The ultimate sources of the fluorine, gold, and other metals is unknown. The deposit is within a regional fluorspar belt which may in part be related to Tertiary volcanic activity (Worl and Griffiths, 1976); mid-Tertiary and younger rhyolites are exposed 8 km west of Relief Canyon. Alternatively, the gold may have been leached from the thick Triassic pelitic sequence, a scenario similar to that proposed for the large Carlin (Radtke et al., 1980) and Jerritt Canyon (Northrop et al., 1987) gold deposits in northern Nevada.

Conclusions

The Relief Canyon gold and fluorite deposit formed in a developing cave and solution breccia system in Triassic limestones and it is probably of late Tertiary age. Ground water partially dissolved the limestones directly beneath their contact with overlying shales and siltstones. Clay and silt particles derived from the shales were transported into the developing cave and breccia zone. Hydrothermal fluids, which were probably introduced along steep normal faults, permeated the cave-fill sediments and may have mixed with the phreatic meteoric waters. Auriferous late-stage jasperoids formed along the fault zones and in irregular blankets at the shale-limestone contact. The sources of the gold and fluorine are unknown; primary magmatic fluids and water circulating through the thick pelitic sequence are possible candidates.

Acknowledgments

The cooperation and support of Lacana Mining, Inc., and Pegasus Gold Corporation have greatly facilitated the field studies for this project. In particular, Clive Bailey of Pegasus and Paul Sonerholm of Lacana, the chief mine geologists during the project, are due special thanks. Rick Mahrt and Gene Whitney provided assistance and advice on clay analyses and their interpretation, Ted Dawes produced the Rock-Eval

analyses on the carbon samples, and Joel Leventhal aided in the interpretation of the carbon data; all are with the U. S. Geological Survey. Warren Day, David Giles, Chuck Patterson, and two *Economic Geology* reviewers improved the manuscript with their reviews.

April 29, October 26, 1988

REFERENCES

- Elison, M. W., and Speed, R. C., 1988, Triassic flysch of the Fencemaker allochthon, East Range, Nevada: Fan facies and provenance: *Geol. Soc. America Bull.*, v. 100, p. 185-199.
- Fiannaca, M. J., and Easdon, M. M., 1984, Problems, solutions, and practical aspects of sampling technique relative to development of the Relief Canyon gold project, Pershing County, Nevada: *Soc. Mining Engineers AIME Preprint* 84-369, 15 p.
- Haas, J. L., Jr., 1971, The effect of salinity on the maximum thermal gradient of a hydrothermal system at hydrostatic pressure: *ECON. GEOL.*, v. 66, p. 940-946.
- Hudson, M. R., and Geissman, J. W., 1987, Paleomagnetic and structural evidence for middle Tertiary counterclockwise block rotation in the Dixie Valley region, west-central Nevada: *Geology*, v. 7, p. 638-642.
- Nichols, K. M., and Silberling, N. J., 1977, Stratigraphy and depositional history of the Star Peak Group (Triassic), northwestern Nevada: *Geol. Soc. America Spec. Paper* 178, 73 p.
- Northrop, H. R., Rye, R. O., Landis, G. P., Lustwerk, R., Jones, M. B., and Daly, W. E., 1987, Sediment-hosted disseminated gold mineralization at Jerritt Canyon, Nevada, V: Stable isotope geochemistry and a model of ore deposition [abs.]: *Geol. Soc. America Abstracts with Programs*, v. 19, p. 791.
- Oldow, J. S., 1984, Evolution of a late Mesozoic back-arc fold and thrust belt, northwestern Great Basin, U.S.A.: *Tectonophysics*, v. 102, p. 245-274.
- Olson, R. A., 1984, Genesis of paleokarst and strata-bound zinc-lead sulfide deposits in a Proterozoic dolostone, northern Baffin Island, Canada: *ECON. GEOL.*, v. 79, p. 1056-1103.
- Papke, K. G., 1979, Fluorspar in Nevada: *Nevada Bur. Mines Geology Bull.* 93, 77 p.
- Potter, R. W., II, 1977, Pressure corrections for fluid-inclusion homogenization temperatures based on the volumetric properties of the system NaCl-H₂O: *U. S. Geol. Survey Jour. Research*, v. 5, p. 603-607.
- Potter, R. W., II, Clynne, M. A., and Brown, D. L., 1978, Freezing point depression of aqueous sodium chloride solutions: *ECON. GEOL.*, v. 73, p. 284-285.
- Radtke, A. S., Rye, R. O., and Dickson, F. W., 1980, Geology and stable isotope studies of the Carlin gold deposit, Nevada: *ECON. GEOL.*, v. 75, p. 641-672.
- Rhodes, D., Lantos, E. A., Lantos, J. A., Webb, R. J., and Owens, D. C., 1984, Pine Point orebodies and their relationship to the stratigraphy, structure, dolomitization, and karstification of the Middle Devonian Barrier Complex: *ECON. GEOL.*, v. 79, p. 991-1055.
- Richardson, C. K., and Holland, H. D., 1979, The solubility of fluorite in hydrothermal solutions, an experimental study: *Geochim. et Cosmochim. Acta*, v. 43, p. 1313-1325.
- Rytuba, J. J., 1985, Geochemistry of hydrothermal transport and deposition of gold and sulfide minerals in Carlin-type gold deposits: *U. S. Geol. Survey Bull.* 1646, p. 27-34.
- Sass-Gustkiewicz, M., 1983, Zinc-lead ore structures from Upper Silesian region in the light of solution transfer, in Kisvarsanyi, C., Grant, S. K., Pratt, W. P., and Koenig, J. W., eds., International conference on Mississippi Valley type lead-zinc deposits. Proceedings volume: Rolla, Univ. Missouri-Rolla Press, p. 20-26.
- Seward, T. M., 1973, Thio complexes of gold and the transport of gold in hydrothermal ore solutions: *Geochim. et Cosmochim. Acta*, v. 37, p. 379-399.
- Silberling, N. J., and Wallace, R. E., 1967, Geologic map of the Imlay quadrangle, Pershing County, Nevada: *U. S. Geol. Survey Geol. Quad. Map GQ-666*, scale 1:62,500.
- 1969, Stratigraphy of the Star Peak Group (Triassic) and overlying lower Mesozoic rocks, Humboldt Range, Nevada: *U. S. Geol. Survey Prof. Paper* 592, 50 p.
- Silberman, M. L., and Berger, B. R., 1985, Relationship of trace-element patterns to alteration and morphology in epithermal precious-metal deposits: *Rev. Econ. Geology*, v. 2, p. 203-232.
- Stewart, J. H., and Carlson, J. E., 1978, Geologic map of Nevada: *U. S. Geol. Survey Map*, scale 1:500,000.
- Tissot, B. P., and Welte, D. H., 1984, Petroleum formation and occurrence, 2nd ed.: New York, Springer-Verlag, 699 p.
- Vikre, P. G., 1984, Paleolandforms above three precious metal deposits in Nevada [abs.]: *Geol. Soc. America Abstracts with Programs*, v. 16, p. 683.
- Vikre, P. G., and McKee, E. H., 1985, Zoning and chronology of hydrothermal events in the Humboldt Range, Pershing County, Nevada: *Isochron/West*, no. 44, p. 17-24.
- Wallace, R. E., Silberling, N. J., Irwin, W. P., and Tatlock, D. B., 1969a, Geologic map of the Buffalo Mountain quadrangle, Pershing and Churchill Counties, Nevada: *U. S. Geol. Survey Geol. Quad. Map GQ-821*, scale 1:62,500.
- Wallace, R. E., Tatlock, D. B., Silberling, N. J., and Irwin, W. P., 1969b, Geologic map of the Unionville quadrangle, Pershing County, Nevada: *U. S. Geol. Survey Geol. Quad. Map GQ-820*, scale 1:62,500.
- Winkler, H. G. F., 1974, Petrogenesis of metamorphic rocks, 3d ed.: New York, Springer-Verlag, 320 p.
- Wittkopp, R. W., Parratt, R. L., and Bruce, W. R., 1984, Geology and mineralization at the Relief Canyon gold deposit, Pershing County, Nevada: *Soc. Mining Engineers AIME Preprint*, 4 p.
- Worl, R. G., and Griffiths, W. R., 1976, Descriptions of major fluorine deposits and districts and important types of fluorine occurrences—Nevada-western Utah-southeastern Oregon-southeastern California-western Arizona: *U. S. Geol. Survey Prof. Paper* 933, p. 41-48.